# Probability of Detection of Defects in Coatings With Electronic Shearography

*S.S. Russell*
*Marshall Space Flight Center • MSFC, Alabama*

*M.D. Lansing, C.M. Horton, W.J. Gnacek*
*University of Alabama in Huntsville*
*Huntsville, Alabama*

June 1995

# TABLE OF CONTENTS

# LIST OF ILLUSTRATIONS

TECHNICAL MEMORANDUM

# PROBABILITY OF DETECTION OF DEFECTS IN COATINGS WITH ELECTRONIC SHEAROGRAPHY

## I. INTRODUCTION

The Systems Management and Production Laboratory at the Research Institute of the University of Alabama in Huntsville was tasked by the Nondestructive Evaluation (NDE) Branch at Marshall Space Flight Center (MSFC) to conduct research in the method of electronic shearography for nondestructive evaluation. The goal of this research was to utilize statistical methods to evaluate the probability of detection (POD) of defects in coatings using electronic shearography. The coating system utilized in the POD studies was to be the paint system currently utilized on the external casings of the NASA space transportation system (STS) reusable solid rocket motor (RSRM) boosters. The population of samples was to be large enough to determine the minimum defect size for 90-percent probability of detection at 95-percent confidence POD on these coatings. Also, the best methods to excite coatings on aerospace components to induce deformations for measurement by electronic shearography were to be determined.

## II. BACKGROUND AND OBJECTIVES

It has been observed that chips of paint occasionally impact the external structure of the space shuttle during and after launch. It is believed that these paint chips originate as debonds in the paint-primer system used on the solid rocket boosters, external tank, or orbiter. The possibility exists for considerable damage to be inflicted upon the vehicle by these high-velocity impacts.

The NDE Branch at MSFC maintains a laboratory for the application and development of the method of electronic shearography. This facility is equipped with a Pratt-Whitney electronic holography/shearography inspection system (PW EH/SIS) and a Laser Technology, Inc., (LTI) SC-4000 (section III.B.1 contains more information on shearography devices). Electronic shearography techniques provide noncontact real-time location and sizing of defects in many material systems. Electronic shearography has proven particularly effective in the evaluation of debonds in laminar material systems, which suggests that the technique should be well suited to the inspection of paint coating systems.

Preliminary to the application of electronic shearography as a field technique to locate and determine the criticality of defects in the STS coating systems, the need was identified to quantify the limitations of the technique for evaluating the type of defects anticipated in those material systems. Also, the methodology for such field evaluation needed to be developed.

The method of performing the POD study was to design and fabricate painted plates containing programmed debonds of various sizes. These panels were then to be inspected in the MSFC NDE Branch Electronic Shearography Laboratory. The results of these inspections would be used to statistically determine the minimum debond size for 90-percent probability of detection with 95-percent confidence.

1

# III. ACTIVITIES

## A. Specimen Design and Fabrication

1. <u>Substrate and Coating Specifications</u>. This project evaluated programmed debonds in the metal substrate and epoxy paint used for the STS RSRM external structure. The substrates utilized were 8- by 12- by 0.25-in thick plates of cold rolled D6AC steel. The coating system was composed of Rust-Oleum™ 9334 epoxy primer undercoat and 9392 flat white epoxy topcoat. The coating was applied per NASA specification STW7-3859 by J&A Finishing, Huntsville, AL. This specification requires a thickness of each of the primer and topcoat between 1.5 and 4 mils. The combined coating thickness was verified by an eddy current method.

2. <u>Debond Simulation</u>

a. <u>Fluid Coupling</u>. Numerous attempts were made to fabricate simulated debonds in the coating systems. All of the initial attempts involved the controlled application of a fluid to the substrate before the paint system was applied. A template was used to screen most of the panel and allow the application of the fluid to regions of prescribed areas. The concept in these debond simulation schemes is that the fluid used prevents the paint from bonding to the steel substrate where the fluid has been applied, thus producing a debond of a programmed size at a predetermined location.

Several fluid types were initially tested, including:

(1) Thompson and Formby Tri-Flow™ spray lubricant with Teflon™

(2) WD-40™ spray lubricant

(3) Permatex Naval Jelly™ rust remover

(4) Conoco HD2™ grease.

Initial testing of the fluids to be used involved the application by hand of a small quantity and covering of the fluid with a coat of spray enamel. The Conoco HD2™ grease was demonstrated to provide the most reliable debond simulation. A series of debond patterns of various sizes were cut from sheets of magnetic vinyl sign material to act as a stencil during grease application. However, problems were encountered in the application of this fluid for programmed debonds.

Thiokol Corporation applied the HD2™ with the Sonotech precision spray facility it maintains at MSFC. The machine was adjusted to provide a very fine coat of grease to simulate contamination for another project and could not be readjusted in the timeframe of this project. The thickest coat that could repeatedly be applied with this technique was 67 mg/ft$^2$. Assuming a uniform application, this quantity of lubricant will result in a layer approximately 0.030-mils thick.

These specimens did not produce debonds detectable by electronic shearography. It is suspected that either the paint was allowed to bond to the steel substrate through the grease or the grease layer was so thin as to create a "kissing debond." A kissing debond occurs when there is no rigid bonding between laminae, but either the material on both sides of the debond is sufficiently thick/stiff to resist influence by the debond or some force such as friction or coupling viscosity prevents the separation of the laminae. That is, the debond physically exists, but the deformation response of the debond to nondamaging

2

excitation is the same as that of a normal bond. Since electronic shearography measures the motion of the specimens' surfaces, it cannot detect debonds that do not respond to excitation differently than the rest of the bonded region.

In the case of these panels, the ratio of the paint thickness to the underlying grease thickness was 4.5 mils/0.0299 mils = 150.5. The fact that the paint was more than 150 times as thick as the grease beneath it indicates that, if the paint over the region of grease is treated as a plate fixed around the edges, there was likely not enough grease to alter the stiffness of the paint above it with respect to the paint around it. Thus, the paint was viscously coupled to the plate surface where the fluid was applied and it behaved the same there as where no fluid was present. This behavior is typical of a kissing debond.

Thicker layers of grease were obtained when panels with the same type of stencils were hand sprayed by AC Engineering. However, the deposited grease was found to be highly nonuniform. The specified target thickness for the grease was 2 to 3 mils. A sufficient volume of grease was applied to produce a uniform layer 2.5-mils thick. However, the rectangular interior of the programmed debonds contained less than 1 mil of grease. The remaining fluid ran, puddled around the edges of the pattern, and seeped beneath the stencil. Thus, instead of a somewhat realistically simulated uniform debond, an unrealistic superposition of a uniform rectangular debond and a rectangular ring-like debond were fabricated. The geometry of these grease regions is depicted in figure 1.

A typical shearogram of these panels, taken with the PW EH/SIS, is shown in figure 2. This shearogram was produced with thermal excitation and indicates that the motion of the thick rings around the uniform debonds is much larger than the motion of the uniform regions themselves. It was not possible to produce enough motion in the thin interior regions that their response would be experimentally or analytically separated from the thick outer rings. Thus, the hand-sprayed panels did not allow for shearographical detection of the programmed uniform rectangular debonds.
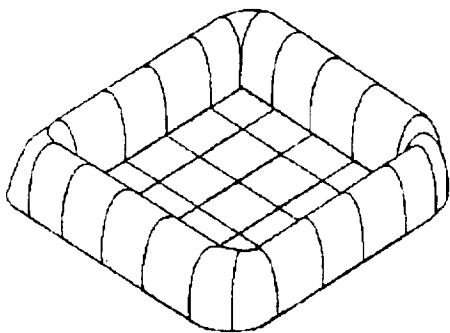


Figure 1.  Hand-sprayed HD2 debond geometry.



Figure 2.  Hand-sprayed HD2 shearogram.

b.  Solid Inserts. After failing to simulate coating debonds with fluids, solid inserts were used. The concept of simulating coating debonds with solid inserts requires that the insert not be bonded to the substrate. The paint applied to the insert then is not bonded to the substrate.

The first inserts tested were single-layer 0.5-mil-thick polymer films. However, the unpainted polymer inserts experienced massive plastic deformation with the slightest application of heat. A similar shriveling response was observed upon application of a thin coat of spray enamel before any heat was

applied. It could not be concluded that a similar reaction would not occur upon application of the RSRM epoxies, and thus the polymer inserts were deemed unsuitable for this study.

The best preliminary results were obtained with single-layer 0.5-mil-thick aluminum foil inserts. The use of these inserts required some form of edge bonding that would prevent the foils from leaving or moving around on the surface of the steel plates during shipping and painting while leaving a region of the foil of known size unbonded to the plate. Initially, hot-melt glue was applied in a very thin bead around all edges of the foil, but this decreased the actual size of the program debonds by an amount that could not be easily determined. Subsequent tests indicated that a small amount of plastic tape ($\cong 1$ by 3 mm) allowed the foils to be anchored around the edges while leaving the entire bottom surface of the foil unbonded.

Square foils of various sizes, ranging from 3 to 24 mm on a side in 3-mm increments were arranged on the surface of the plates before painting. Table 1 shows the programmed debond sizes. The foils were placed with plastic tape as shown in figure 3. The arrangement of foils is shown in figure 4. Each painted plate contains seven debonds of each of the eight program debond sizes. Two identical panels were prepared, providing a total of 112 physical debonds.

Table 1. Programmed debond sizes (mm).

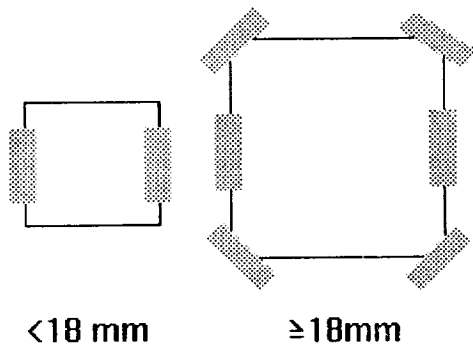|   | A,C,E | B,D,F | G |   |   | A,C,E, | B,D,F | G |
|---|-------|-------|---|---|---|--------|-------|---|
| 1 | 24 | 3 | 21 |   | 5 | 18 | 9 | 6 |
| 2 | 6 | 21 | 15 |   | 6 | 12 | 15 | 12 |
| 3 | 18 | 9 | 9 |   | 7 | 21 | 6 | 18 |
| 4 | 12 | 15 | 3 |   | 8 | 3 | 24 | 24 |



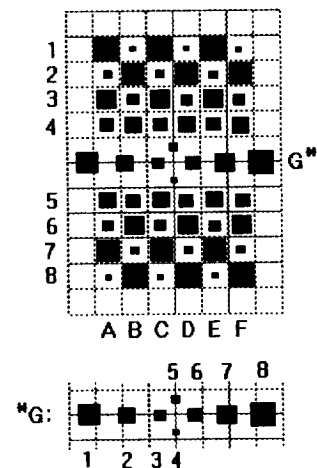Figure 3. Foil placement with plastic tape.



Figure 4. Foil insert programmed debond pattern.

## B. Data Acquisition

1. Apparatus. The MSFC NDE Branch Electronic Shearography Laboratory is equipped with two electronic shearography instruments. The LTI SC-4000 utilizes a birefringent lens to induce a fixed

4

shearing angle (LTI patent No. 4,887,899). The shear distance is thus predetermined by the distance from the object to the shearography camera. The shear distance is 0.75 inch at an object distance of 8 ft. This system produces basic shearograms that are the superposition of a single undeformed and a single deformed image, each of which is the superposition of two sheared images at the same deformation state. For more information on the technique of electronic shearography, see references 1 through 12.

The PW EH/SIS utilizes a modified Michelson interferometer (LTI patent No. 5,094,528) and provides several image enhancement functions. Frame averaging acquires a series of images at each deformation state. The number of images acquired is user defined. At each deformation stage, the mean intensity of each pixel over the range of frames is used to produce a frame-averaged image. This function sharpens the features of the object surface and reduces noise.

Speckle averaging with the PW EH/SIS employs a stepper motor-driven etalon to rotate the illumination beam, and thus the laser speckle pattern on the object, by 90° between image series. That is, a series of images is acquired at each beam rotation and averaged to produce the image at each deformation state. The total number of frames that are averaged to produce each image is thus four times the number of frames to be averaged. Speckle averaging produces sharper fringes and reduces noise.

The PW EH/SIS allows the user to place labels and pointers on the image as graphics. A video caliper is also provided that may be calibrated to real-world coordinates and allows for the on-screen measurement of detection sizes.

The LTI SC-4000 was less useful in the evaluation of the test plates, due to its high shear angle, than was the variable shear angle PW EH/SIS. The former system was intended for use in the detection of large structural delaminations and damage. Also, the image-enhancing capabilities of the PW EH/SIS facilitated the detection of small debonds in coatings. The LTI shearogram in figure 5 may be compared to the PW shearograms in the appendix for the same plate, all of which utilized thermal excitation. Thus, the PW EH/SIS was utilized for this probability of detection study.



Figure 5. LTI SC-4000 shearogram of panel 25.
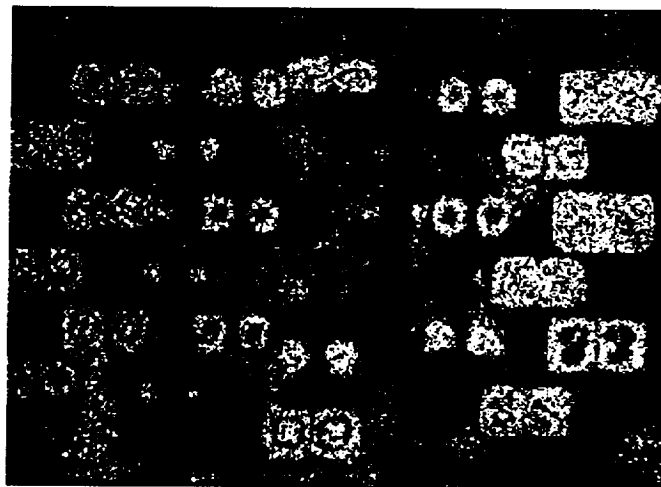
The PW EH/SIS acquires the electronic shearograms as digital images via an NEC TI-23A charge-coupled device (CCD) camera with a 480- by 512-pixel resolution. This camera is equipped with a 12.5- to 75-mm telephone lens. The shearograms are displayed on a Sony PVM-1342Q video monitor, and hard copies are produced by a Sony VP3000 video printer. Object illumination is supplied by Adlas

DPY325C light-emitting diode (LED) pumped-frequency doubled-neodymium-doped yttrium-aluminum garnet (ND:YAG) laser with a power rating of 140 mW at a wavelength of 532 nm.

2. Procedure. The painted plates were thermally excited to induce debond motion. The plates were lightly heated from the front with a hand-held heat gun. The undeformed images were captured while the plate was still hot, and the deformed images were acquired after it had cooled. That is, the measured deformation was thermal contraction associated with the cooling of the material system.

The PW EH/SIS lens was oriented 8 ft from the surface of the test panels. The zoom lens was used to adequately fill the field-of-view with the test panel image while allowing the best focus. Each test panel was inspected individually. Frame averaging was used with the number of frames set to four. Speckle averaging was also used, and optional traveling fringes were not displayed. The image shearing distance was adjusted to 2-mm horizontal.

The data was acquired in the form of electronic shearogram video images. The video caliper was used to measure the size of each detection in the vertical direction. Each of three inspectors acquired two shearograms of each plate. This resulted in 672 debond size measurements. That is, there were 84 observations of each of the 8 standard debond sizes. The shearograms and measurements are included in the appendix.

## C. Analysis

The measured sizes of the detected debonds were analyzed numerically by the POD software system (POD/SS) AHAT routine (A.P. Berens, P.W. Hovey, R.M. Donahue, and W.N. Craport, University of Dayton Research Institute, 1988). This software fits a POD curve of the form $\ln(\hat{\alpha}) = \beta_1 + \beta_2 \ln(\alpha)$ where $\hat{\alpha}$ values are the measured debond sizes and $\alpha$ values are the standard debond sizes.

## D. Results

The results of the POD/SS analysis are shown in figures 6 and 7. It was found that the POD of detection is greater than 90 percent if the debond size is greater than 9.95 mm. However, in order to achieve 95-percent confidence, the debond size must be greater than 15.62 mm.
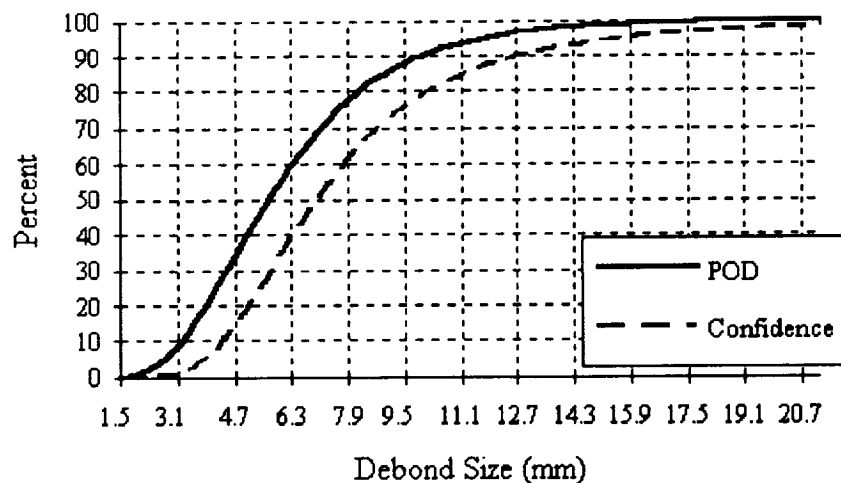


Figure 6. Electronic shearography POD of debonds in coatings (90/95:15.62 mm).
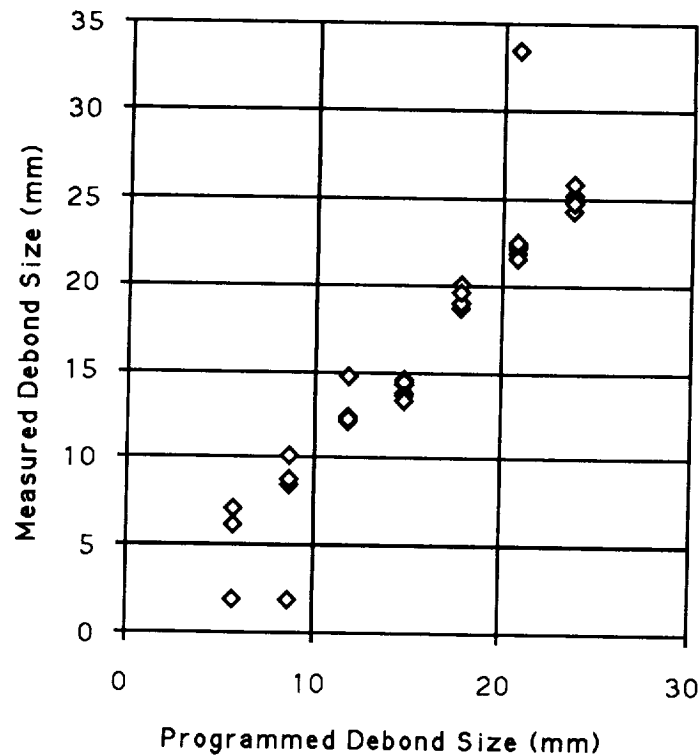
Figure 7. Electronic shearography coating debond size measurement scatter.

The field-of-view in this experiment was approximately 305-mm (12-in) wide. Thus the minimum 90/95 detection size is approximately 5.1 percent of the field-of-view. These results may be compared with a POD study conducted by LTI for an aluminum honeycomb aerospace battery housing (see reference 6). It was determined that the minimum flaw size for 90/95 detection was 7.16 mm (0.282 in) with a field-of-view 127-mm (5-in) wide. Thus, the minimum size is approximately 5.6 percent of the field-of-view. These results compliment each other despite the different apparatus, material systems, and geometries involved.

## IV. DISCUSSION

The minimum debond size for 90-percent POD with 95-percent confidence is dependent upon several parameters. For example, while the minimum size in this study was found to be about 5 percent of the field-of-view, this proportion is dependent on the size of the field-of-view. That is, if the same setup and analysis, including a 2-mm shear distance, were used with a 4- by 6-ft field-of-view, the minimum size cannot be extrapolated to be 5 percent × 6 ft = 3.6 in. The minimum debond size is also dependent on the image shearing distance, which is in turn dependent on the object distance and image shearing angle. Even if the shearing angle is kept the same, allowing the shearing distance to change, this type of extrapolation does not hold. If any procedure other than that described is to be used, a POD study must be conducted for that procedure.

The procedure used in this study was confined to the analysis of debonds on the 8- by 12-in plates provided by NASA. If it is desired to conduct electronic shearography inspection for coating debonds over a large surface, i.e., the entire surface of an RSRM, then, in the interest of time and expense, it may be preferable to evaluate a larger area with each inspection. For the reasons explained,

7

and because debonds on a large curve structure will exhibit different detections than those on a flat plate, a POD analysis should be conducted on specimens which more closely resemble the area and curvature of the RSRM. However, the deviations associated with size and curvature may be simultaneously overcome by the development of an automated robotic or computer numerically controlled electronic shearography system. Even if larger areas are to be inspected, the simplest form of such an automated system would significantly decrease the time, and perhaps long-term expense, required to inspect such a large structure.

Electronic shearography fringe orders may be related to changes in surface slopes by the equation (derived in reference 5):

$$\partial w/\partial x = \lambda/2s \ .$$

For this study, a shearing distance, $s$, of 2 mm was used. The PW EH/SIS laser provides illumination with a wavelength, $\lambda$, of 532 nm. From the equation above, each fringe in the resulting shearograms represents a change in surface slope of 0.133 mm/m. This may be expressed as an angle of 0.000133 radians or $0.00762°$.

# V. CONCLUSIONS

Debonds of sizes 3 to 24 mm were simulated with aluminum foil inserts on 8- by 12-in plates of the RSRM coating/substrate material system. A total of 84 observations of each of the 8 debond sizes were obtained with electronic shearography. The size of these detections were numerically analyzed. It was determined that, with the experimental parameters and procedures used, electronic shearography provides 90-percent probability of detection at 95-percent confidence for all debond sizes greater than 16.52 mm, or approximately 5 percent of the field-of-view width.

**APPENDIX**

Panel 25
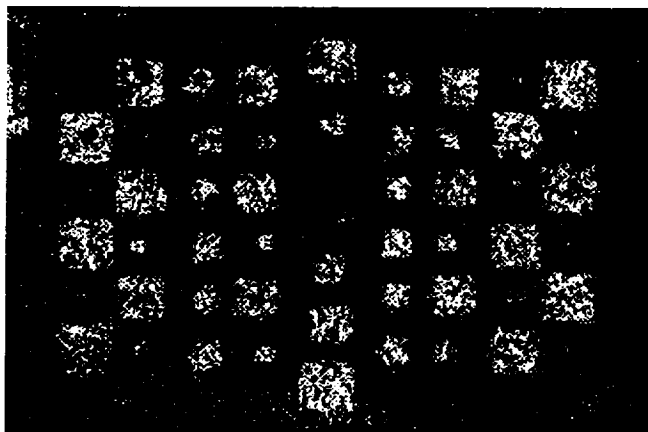


Inspection B25-1
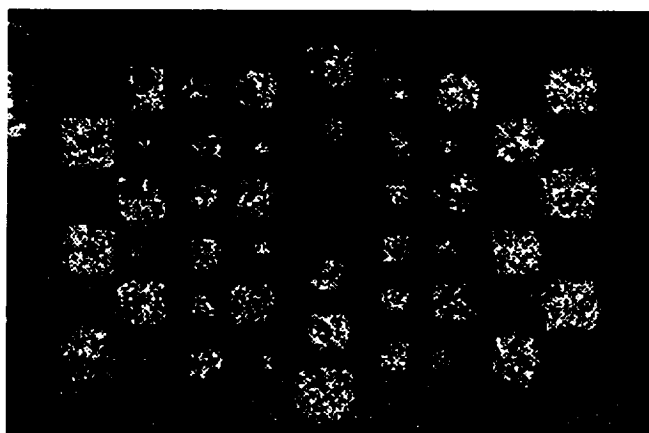
Inspection B25-2



Inspection M25-1

Inspection M25-2



Inspection P25-1

Inspection P25-2

11

Panel 26



Inspection B26-1



Inspection B26-2



Inspection M26-1



Inspection M26-2



Inspection P26-1



Inspection P26-2

12

PW EH/SIS Debond Size Measurements

Panel 25

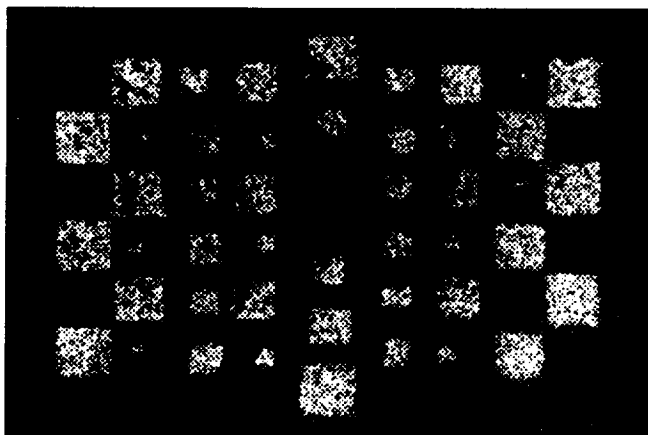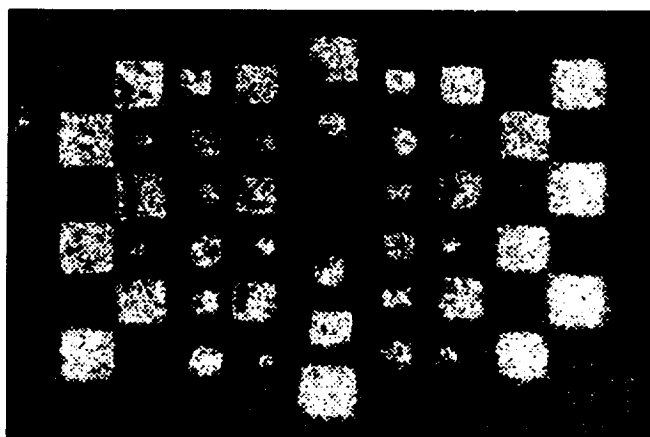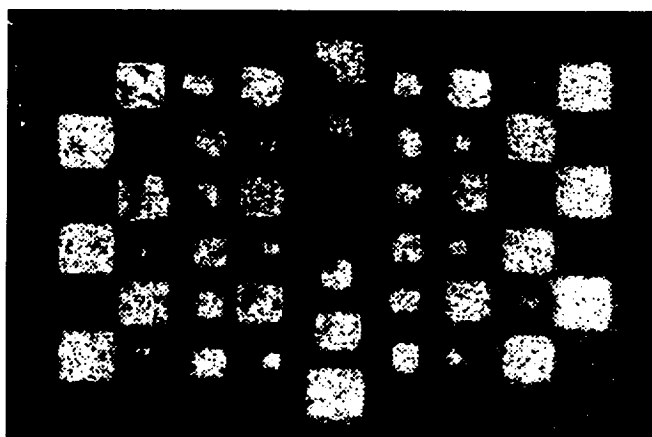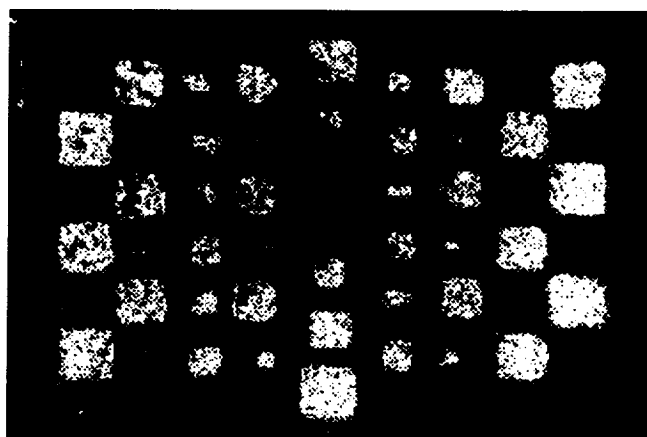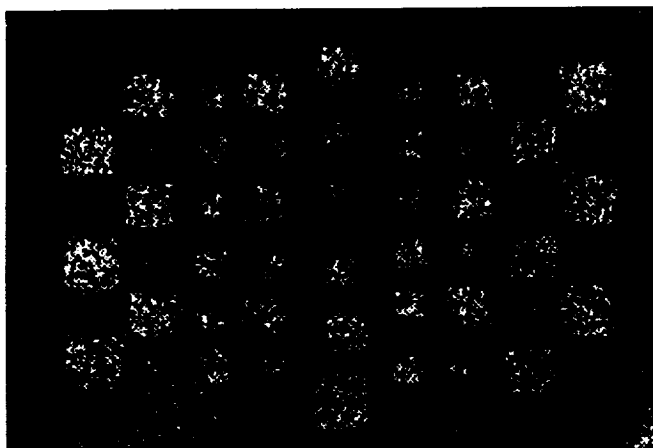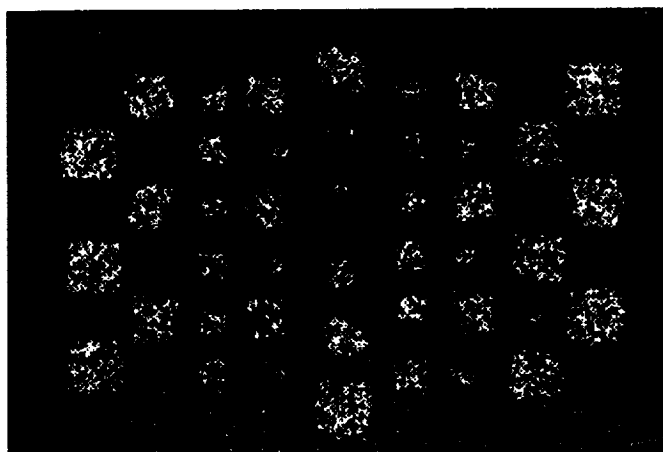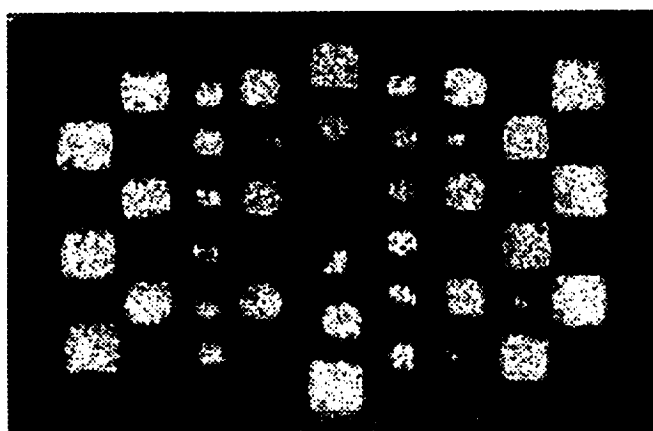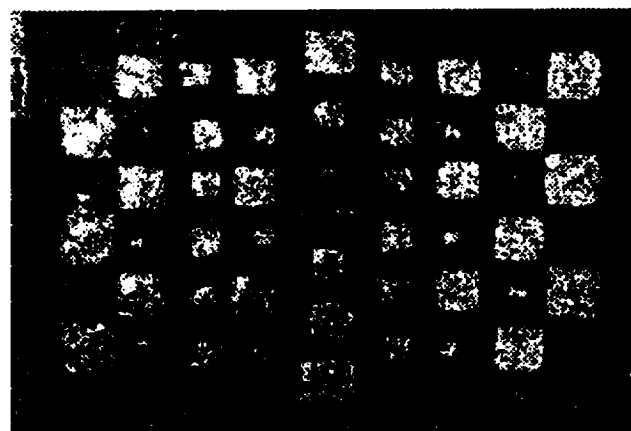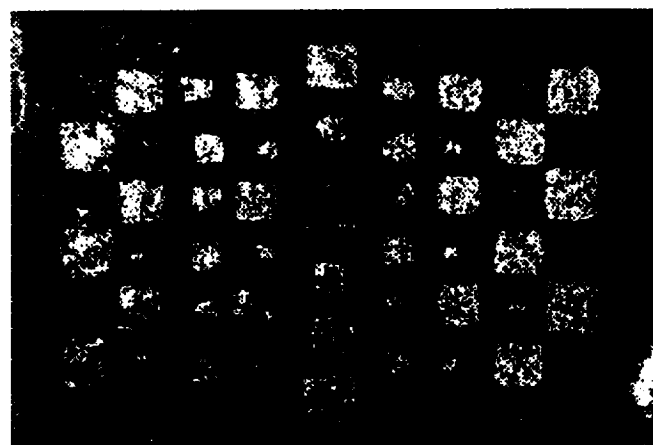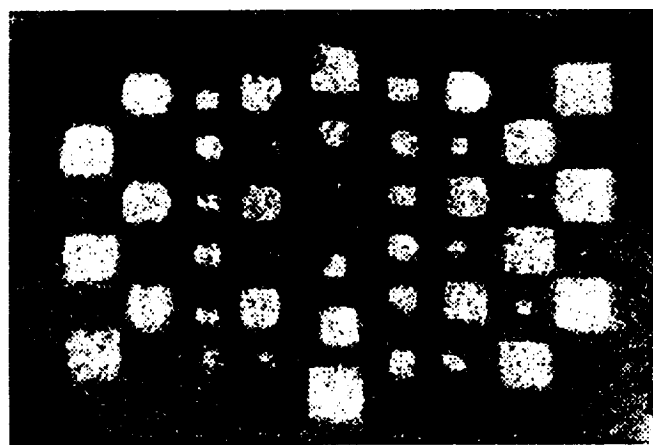| Name | Size | B25-1 | B25-2 | M25-1 | M25-2 | P25-1 | P25-2 |
|------|------|-------|-------|-------|-------|-------|-------|
| A1 | 24 | 23.09 | 24.10 | 23.09 | 23.10 | 23.26 | 21.84 |
| A2 | 6 | 0.00 | 0.00 | 2.57 | 0.00 | 3.80 | 0.00 |
| A3 | 18 | 19.51 | 18.97 | 17.44 | 17.40 | 18.52 | 17.09 |
| A4 | 12 | 13.84 | 12.83 | 11.29 | 12.30 | 12.34 | 9.02 |
| A5 | 18 | 18.97 | 18.97 | 17.96 | 18.50 | 18.99 | 17.57 |
| A6 | 12 | 14.88 | 15.90 | 11.80 | 13.80 | 10.92 | 10.45 |
| A7 | 21 | 22.07 | 21.03 | 21.55 | 22.10 | 21.84 | 21.84 |
| A8 | 3 | 0.00 | 0.00 | 0.00 | 0.00 | 0.00 | 0.00 |
| B1 | 3 | 0.00 | 0.00 | 0.00 | 0.00 | 0.00 | 0.00 |
| B2 | 21 | 20.52 | 22.07 | 22.06 | 22.60 | 22.31 | 21.84 |
| B3 | 9 | 14.38 | 12.83 | 8.21 | 11.30 | 10.92 | 7.60 |
| B4 | 15 | 15.39 | 14.88 | 13.34 | 14.90 | 14.72 | 14.24 |
| B5 | 9 | 8.71 | 7.70 | 7.70 | 9.25 | 7.60 | 6.17 |
| B6 | 15 | 13.34 | 13.84 | 13.85 | 13.80 | 14.24 | 13.23 |
| B7 | 6 | 0.00 | 5.64 | 4.10 | 7.19 | 5.70 | 0.00 |
| B8 | 24 | 25.65 | 24.10 | 24.63 | 24.60 | 24.21 | 24.21 |
| C1 | 224 | 25.15 | 26.16 | 23.60 | 25.10 | 24.21 | 23.74 |
| C2 | 6 | 0.00 | 0.00 | 4.10 | 0.00 | 0.00 | 0.00 |
| C3 | 18 | 21.03 | 20.02 | 16.93 | 19.50 | 18.99 | 18.99 |
| C4 | 12 | 12.32 | 14.88 | 11.80 | 10.80 | 11.39 | 8.55 |
| C5 | 18 | 18.47 | 20.02 | 17.96 | 18.00 | 18.52 | 18.52 |
| C6 | 12 | 14.38 | 11.81 | 12.31 | 12.90 | 11.39 | 10.45 |
| C7 | 21 | 22.07 | 21.54 | 21.04 | 20.50 | 21.36 | 22.31 |
| C8 | 3 | 0.00 | 0.00 | 0.00 | 0.00 | 0.00 | 0.00 |
| D1 | 3 | 0.00 | 0.00 | 0.00 | 0.00 | 0.00 | 0.00 |
| D2 | 21 | 23.09 | 21.54 | 21.04 | 21.50 | 21.36 | 21.36 |
| D3 | 9 | 12.32 | 8.71 | 9.24 | 8.71 | 8.55 | 6.17 |
| D4 | 15 | 14.88 | 13.84 | 13.85 | 13.30 | 14.24 | 13.77 |
| D5 | 9 | 9.75 | 8.71 | 8.72 | 9.25 | 7.60 | 5.70 |
| D6 | 15 | 14.38 | 14.88 | 13.85 | 12.80 | 14.72 | 14.72 |
| D7 | 6 | 8.71 | 5.13 | 4.10 | 6.68 | 6.17 | 6.65 |
| D8 | 24 | 24.10 | 24.10 | 23.09 | 23.10 | 23.74 | 23.26 |
| E1 | 24 | 25.65 | 24.10 | 23.60 | 25.10 | 23.26 | 24.21 |
| E2 | 6 | 7.70 | 0.00 | 0.00 | 0.00 | 6.17 | 0.00 |
| E3 | 18 | 18.97 | 21.54 | 18.47 | 20.50 | 19.94 | 19.47 |
| E4 | 12 | 13.84 | 12.83 | 9.24 | 11.30 | 11.87 | 10.45 |
| E5 | 18 | 21.54 | 20.52 | 18.98 | 18.50 | 18.99 | 18.99 |
| E6 | 12 | 16.41 | 12.32 | 12.83 | 14.40 | 14.24 | 12.82 |
| E7 | 21 | 21.03 | 20.52 | 20.52 | 20.00 | 20.42 | 20.89 |
| E8 | 3 | 0.00 | 0.00 | 0.00 | 0.00 | 0.00 | 0.00 |
| F1 | 3 | 0.00 | 0.00 | 0.00 | 0.00 | 0.00 | 0.00 |
| F2 | 21 | 23.09 | 22.58 | 21.04 | 22.80 | 22.34 | 21.36 |

13

| Name | Size | B25-1 | B25-2 | M25-1 | M25-2 | P25-1 | P25-2 |
|------|------|-------|-------|-------|-------|-------|-------|
| F3 | 9 | 13.84 | 10.77 | 9.75 | 10.30 | 9.02 | 9.50 |
| F4 | 15 | 15.39 | 14.88 | 13.34 | 12.30 | 13.29 | 15.67 |
| F5 | 9 | 8.71 | 8.71 | 7.70 | 8.71 | 8.55 | 9.02 |
| F6 | 15 | 15.39 | 14.38 | 12.31 | 13.80 | 13.77 | 14.72 |
| F7 | 6 | 9.75 | 0.00 | 4.62 | 0.00 | 4.75 | 0.00 |
| F8 | 24 | 24.10 | 24.64 | 22.58 | 25.10 | 22.79 | 23.74 |
| G1 | 21 | 23.09 | 22.58 | 19.50 | 21.00 | 21.37 | 20.89 |
| G2 | 15 | 13.34 | 13.34 | 13.34 | 13.30 | 11.87 | 9.50 |
| G3 | 9 | 0.00 | 0.00 | 0.00 | 0.00 | 0.00 | 0.00 |
| G4 | 3 | 0.00 | 0.00 | 0.00 | 0.00 | 0.00 | 0.00 |
| G5 | 6 | 4.62 | 0.00 | 0.00 | 0.00 | 0.00 | 0.00 |
| G6 | 12 | 14.88 | 15.39 | 14.88 | 16.40 | 14.72 | 15.19 |
| G7 | 18 | 20.52 | 18.47 | 18.98 | 18.50 | 18.52 | 18.52 |
| G8 | 24 | 26.70 | 24.64 | 24.11 | 24.60 | 24.21 | 24.21 |

Panel 26

| Name | Size | B26-1 | B26-2 | M26-1 | M26-2 | P26-1 | P26-2 |
|------|------|-------|-------|-------|-------|-------|-------|
| A1 | 24 | 24.64 | 25.67 | 25.31 | 23.71 | 25.65 | 26.16 |
| A2 | 6 | 0.00 | 0.00 | 4.40 | 2.82 | 0.00 | 0.00 |
| A3 | 18 | 21.05 | 18.99 | 19.26 | 18.63 | 20.52 | 20.02 |
| A4 | 12 | 11.81 | 13.35 | 11.55 | 11.85 | 11.81 | 13.34 |
| A5 | 18 | 18.99 | 21.05 | 18.71 | 17.50 | 15.90 | 18.47 |
| A6 | 12 | 13.86 | 14.89 | 12.65 | 11.85 | 7.70 | 10.26 |
| A7 | 21 | 21.05 | 21.56 | 20.91 | 22.58 | 22.07 | 20.52 |
| A8 | 3 | 0.00 | 0.00 | 0.00 | 0.00 | 0.00 | 0.00 |
| B1 | 3 | 0.00 | 0.00 | 0.00 | 0.00 | 0.00 | 0.00 |
| B2 | 21 | 21.05 | 22.59 | 21.46 | 22.01 | 22.07 | 22.58 |
| B3 | 9 | 11.29 | 8.73 | 8.25 | 9.03 | 9.75 | 9.25 |
| B4 | 15 | 14.89 | 16.43 | 11.00 | 14.11 | 14.88 | 13.84 |
| B5 | 9 | 11.81 | 9.24 | 8.80 | 9.03 | 7.19 | 7.19 |
| B6 | 15 | 13.86 | 14.37 | 12.65 | 14.68 | 12.83 | 12.32 |
| B7 | 6 | 6.67 | 0.00 | 0.00 | 0.00 | 0.00 | 0.00 |
| B8 | 24 | 25.67 | 26.18 | 25.31 | 24.84 | 25.15 | 25.15 |
| C1 | 224 | 25.67 | 24.64 | 26.96 | 25.40 | 26.16 | 26.16 |
| C2 | 6 | 7.19 | 0.00 | 4.40 | 4.52 | 7.19 | 5.13 |
| C3 | 18 | 21.56 | 18.48 | 19.81 | 19.19 | 20.52 | 20.01 |
| C4 | 12 | 13.35 | 13.35 | 13.20 | 11.85 | 11.81 | 11.81 |
| C5 | 18 | 17.97 | 18.48 | 18.71 | 20.32 | 18.97 | 18.47 |
| C6 | 12 | 12.83 | 10.27 | 9.35 | 11.85 | 11.81 | 9.75 |
| C7 | 21 | 20.53 | 20.53 | 21.46 | 21.45 | 22.07 | 21.03 |
| C8 | 3 | 0.00 | 0.00 | 0.00 | 3.95 | 0.00 | 0.00 |
| D1 | 3 | 0.00 | 0.00 | 1.65 | 0.00 | 0.00 | 0.00 |
| D2 | 21 | 22.59 | 22.59 | 22.01 | 21.45 | 22.58 | 23.60 |
| D3 | 9 | 11.29 | 9.75 | 7.15 | 6.21 | 7.19 | 8.71 |

| Name | Size | B26-1 | B26-2 | M26-1 | M26-2 | P26-1 | P26-2 |
|------|------|-------|-------|-------|-------|-------|-------|
| D4 | 15 | 14.89 | 13.86 | 13.20 | 12.98 | 14.88 | 14.88 |
| D5 | 9 | 10.78 | 8.73 | 0.00 | 7.90 | 7.19 | 0.00 |
| D6 | 15 | 16.43 | 13.86 | 13.20 | 11.68 | 12.83 | 10.77 |
| D7 | 6 | 0.00 | 0.00 | 0.00 | 5.08 | 0.00 | 0.00 |
| D8 | 24 | 24.64 | 26.18 | 25.31 | 24.27 | 24.64 | 23.60 |
| E1 | 24 | 24.64 | 25.67 | 25.31 | 24.84 | 25.15 | 25.65 |
| E2 | 6 | 7.19 | 6.16 | 6.05 | 6.21 | 8.20 | 7.19 |
| E3 | 18 | 19.51 | 19.51 | 19.81 | 20.32 | 20.01 | 20.01 |
| E4 | 12 | 11.81 | 12.83 | 13.20 | 12.42 | 11.28 | 12.32 |
| E5 | 18 | 19.51 | 21.05 | 20.91 | 19.19 | 20.01 | 20.02 |
| E6 | 12 | 11.81 | 10.78 | 11.00 | 12.42 | 9.25 | 8.71 |
| E7 | 21 | 21.56 | 23.10 | 23.11 | 22.01 | 22.07 | 21.54 |
| E8 | 3 | 0.00 | 0.00 | 0.00 | 0.00 | 0.00 | 0.00 |
| F1 | 3 | 0.00 | 0.00 | 0.00 | 0.00 | 0.00 | 0.00 |
| F2 | 21 | 22.08 | 23.10 | 24.21 | 22.01 | 23.60 | 23.60 |
| F3 | 9 | 12.32 | 10.78 | 8.25 | 9.50 | 7.19 | 9.25 |
| F4 | 15 | 16.94 | 14.37 | 12.65 | 13.55 | 14.38 | 14.38 |
| F5 | 9 | 9.75 | 9.24 | 9.90 | 7.34 | 8.20 | 7.70 |
| F6 | 15 | 14.89 | 14.37 | 12.10 | 14.11 | 14.38 | 8.71 |
| F7 | 6 | 0.00 | 0.00 | 0.00 | 4.52 | 0.00 | 0.00 |
| F8 | 24 | 25.67 | 25.67 | 26.41 | 24.27 | 25.15 | 25.65 |
| G1 | 21 | 23.10 | 23.62 | 23.11 | 22.01 | 24.10 | 22.58 |
| G2 | 15 | 15.40 | 14.37 | 14.86 | 12.98 | 12.32 | 13.84 |
| G3 | 9 | 11.29 | 6.67 | 0.00 | 3.95 | 5.13 | 5.64 |
| G4 | 3 | 0.00 | 0.00 | 0.00 | 2.82 | 0.00 | 0.00 |
| G5 | 6 | 5.65 | 0.00 | 0.00 | 2.26 | 4.62 | 0.00 |
| G6 | 12 | 14.37 | 14.89 | 12.10 | 14.68 | 13.84 | 13.32 |
| G7 | 18 | 20.53 | 20.53 | 21.46 | 19.19 | 19.51 | 20.52 |
| G8 | 24 | 27.21 | 26.70 | 27.51 | 24.84 | 26.70 | 26.16 |

# REFERENCES

1. Boone, P.M.: "Determination of Slope and Strain Contours by Double-Exposure Shearing Interferometry." *Experimental Mechanics*, August 1975.

2. Engel, J.E., and Burleigh, D.D.: "Validation of Laser Shearography Testing for Fixed Foam Insulation Bonds." *Review of Progress in Quantitative Nondestructive Evaluation*, vol. 9, 1990.

3. Hung, Y.Y.: "Shearograhy: A New Optical Method for Strain Measurement and Nondestructive Testing." *Optical Engineering*, May/June 1982.

4. Hung, Y.Y.: "Shearography: A New Strain-Measurement Technique and a Practical Approach to Nondestructive Testing." *SEM Manual on Experimental Methods for Mechanical Testing of Composites*, 1989.

5. Lansing, M.D., and Workman, G.A.: "Theory and Application of Electronic Shearography." Final Technical Report for NASA DO99, August 1994.

6. Laser Technology, Inc.: "Advanced Shearography NDT," May 25, 1994.

7. Mohanty, R.K., Joenathan, C., and Sirohi, R.S.: "Speckle and Speckle-Shearing Interferometers Combined for the Simultaneous Determination of Out-of-Plane Displacement and Slope." *Applied Optics*, September 15, 1985.

8. Mohanty, R.K., Joenathan, C., and Sirohi, R.S.: "High Sensitivity Tilt Measurement by Speckle Shear Interferometry." *Applied Optics*, May 15, 1986.

9. Newman, J.W.: "Inspection of Aircraft Structure With Advanced Shearography." 1990 ASNT Fall Conference, October 10, 1990.

10. Owner-Peterson, M.: "Digital Speckle Pattern Shearing Interferometry: Limitations and Prospects." *Applied Optics*, July 1, 1991.

11. Tay, C.J., Chau, F.S., Shang, H.M., Shim, V.P.W., and Toh, S.L.: "The Measurement of Slope Using Shearography." *Optics and Lasers in Engineering*, 1990.

12. Toh, S.L., Shang, H.M., Chau, F.S., and Tay, C.J.: "Flaw Detection in Composites Using Time-Average Shearography." *Optics and Laser Technology*, vol. 23, No. 1, 1991.
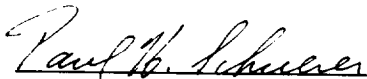
# APPROVAL

## PROBABILITY OF DETECTION OF DEFECTS IN COATINGS WITH ELECTRONIC SHEAROGRAPHY

By S. Russell, M. Lansing, C. Horton, and W. Gnacek

The information in this report has been reviewed for technical content. Review of any information concerning Department of Defense or nuclear energy activities or programs has been made by the MSFC Security Classification Officer. This report, in its entirety, has been determined to be unclassified.


M.R. CARRUTH
Chief, Engineering Physics Division


P.H. SCHUERER
Director, Materials and Processes Laboratory

# REPORT DOCUMENTATION PAGE

Public reporting burden for this collection of information is estimated to average 1 hour per response, including the time for reviewing instructions, searching existing data sources, gathering and maintaining the data needed, and completing and reviewing the collection of information. Send comments regarding this burden estimate or any other aspect of this collection of information, including suggestions for reducing this burden, to Washington Headquarters Services, Directorate for Information Operations and Reports, 1215 Jefferson Davis Highway, Suite 1204, Arlington, VA 22202-4302, and to the Office of Management and Budget, Paperwork Reduction Project (0704-0188), Washington, DC 20503.

| 1. AGENCY USE ONLY (Leave blank) | 2. REPORT DATE | 3. REPORT TYPE AND DATES COVERED |
|---|---|---|
| | June 1995 | Technical Memorandum |

**4. TITLE AND SUBTITLE**

Probability of Detection of Defects in Coatings With Electronic Shearography

**5. FUNDING NUMBERS**

**6. AUTHOR(S)**

S.S. Russell, M.D. Lansing,* C.M. Horton,* and W.J. Gnacek*

**7. PERFORMING ORGANIZATION NAME(S) AND ADDRESS(ES)**

George C. Marshall Space Flight Center
Marshall Space Flight Center, Alabama 35812

**8. PERFORMING ORGANIZATION REPORT NUMBER**

**9. SPONSORING/MONITORING AGENCY NAME(S) AND ADDRESS(ES)**

National Aeronautics and Space Administration
Washington, DC 20546

**10. SPONSORING/MONITORING AGENCY REPORT NUMBER**

NASA TM–108493

**11. SUPPLEMENTARY NOTES**

Prepared by Materials and Processes Laboratory, Science and Engineering Directorate.
*University of Alabama in Huntsville, Huntsville, AL.

**12a. DISTRIBUTION/AVAILABILITY STATEMENT**

Unclassified – Unlimited
Subject Category 24

**12b. DISTRIBUTION CODE**

**13. ABSTRACT (Maximum 200 words)**

The goal of this research was to utilize statistical methods to evaluate the probability of detection (POD) of defects in coatings using electronic shearography. The coating system utilized in the POD studies was to be the paint system currently utilized on the external casings of the NASA space transportation system reusable solid rocket motor boosters. The population of samples was to be large enough to determine the minimum defect size for 90-percent POD of 95-percent confidence POD on these coatings. Also, the best methods to excite coatings on aerospace components to induce deformations for measurement by electronic shearography were to be determined.

**14. SUBJECT TERMS**

shearography, probability of detection

**15. NUMBER OF PAGES**

18

**16. PRICE CODE**

NTIS

| 17. SECURITY CLASSIFICATION OF REPORT | 18. SECURITY CLASSIFICATION OF THIS PAGE | 19. SECURITY CLASSIFICATION OF ABSTRACT | 20. LIMITATION OF ABSTRACT |
|---|---|---|---|
| Unclassified | Unclassified | Unclassified | Unlimited |

NSN 7540-01-280-5500

Standard Form 298 (Rev. 2-89)
Prescribed by ANSI Std. Z39-18